

# Phase Behavior of Lipid Monolayers Containing DPPC and Cholesterol Analogs

Benjamin L. Stottrup and Sarah L. Keller

Departments of Physics and Chemistry, University of Washington, Seattle, Washington 98195

**ABSTRACT** We investigate the miscibility phase behavior of lipid monolayers containing a wide variety of sterols. Six of the sterols satisfy a definition from an earlier study of “membrane-active sterols” in bilayers (cholesterol, epicholesterol, lathosterol, dihydrocholesterol, ergosterol, and desmosterol), and six do not (25-hydroxycholesterol, lanosterol, androstenolone, coprostanol, cholestane, and cholestenone). We find that monolayers containing dipalmitoyl phosphatidylcholine mixed with membrane-active sterols generally produce phase diagrams containing two distinct regions of immiscible liquid phases, whereas those with membrane-inactive sterols generally do not. This observation establishes a correlation between lipid monolayers and bilayers. It also demonstrates that the ability to form two regions of immiscibility in monolayers is not one of the biophysical attributes that explains cholesterol’s predominance in animal cell membranes. Furthermore, we find unusual phase behavior for dipalmitoyl phosphatidylcholine monolayers containing 25-hydroxycholesterol, which produce both an upper and a lower miscibility transition. The lower transition correlates with a sharp change of slope in the pressure-area isotherm.

## INTRODUCTION

A wide array of sterols is found in cell membranes throughout the plant and animal kingdoms (1). In humans, cholesterol is a major component of cell plasma membranes, contributing as much as 50 mol % of the lipid composition (2). The addition of cholesterol to phospholipid bilayers has biophysical effects of altering membrane rigidity, of increasing *sn*-1 lipid chain order, of inhibiting membrane permeability, and of inducing liquid-liquid phase separation (3–6).

Cholesterol biosynthesis progresses along a pathway from lanosterol to cholesterol. Although cholesterol is believed to have superior biophysical properties compared to its precursor sterols (2,5,7,8), it is unknown which of these membrane properties is most responsible for the predominance of cholesterol with respect to other sterols. Missteps in the cholesterol synthesis pathway result in debilitating human diseases such as Smith-Lemli-Opitz syndrome, desmosterolosis, and CHILD syndrome (9). In animal models, inhibition of cholesterol synthesis results in retinal degradation and limb malformation (10,11).

Clearly, the biochemical properties of cholesterol are as important as the biophysical properties (12). For example, cholesterol is a precursor for several critical hormones (9). Studies such as ours that compare a variety of different sterols by measuring membrane lipid packing and miscibility phase behavior are motivated by a desire to decouple the biophysical and biochemical roles of cholesterol in living organisms. If the biophysical requirements of cholesterol are well understood and can be mimicked by other sterols, it may be possible to tease out the purely biochemical roles of cholesterol (13).

Our laboratory has studied model vesicle systems containing lipids and cholesterol in which micron-scale liquid domains appear in the membrane over a wide range of temperatures and ternary compositions (14–16). Recently, our lab and others have substituted alternate sterols for cholesterol in vesicles (17,18). We have found that sterols that produce two liquid phases in phospholipid vesicle membranes generally fit the definition of “membrane-active” sterols proposed by Barenholz in 2002 (19). Membrane-active sterols have a flat structure of fused rings, a hydroxyl headgroup, an alkyl tail, and a monolayer molecular area below 40 Å<sup>2</sup> at a surface pressure of 12 mN/m. Barenholz defines natural membrane-active sterols as decreasing membrane permeability, increasing order in the lipid acyl chains near the terminal methyl group, and enabling the growth of sterol auxotroph microorganisms (19).

Lipids and sterols also demix into coexisting liquid phases when self-assembled in a monolayer at the air-water interface. Fig. 1 outlines three types of monolayer miscibility phase diagrams found in the literature. Early work reported only one region of coexisting liquid phases at low pressure (20). Subsequent work in similar systems has described distinct regions of immiscibility at low cholesterol (the  $\alpha$ -region) and high cholesterol (the  $\beta$ -region) (21,22). Two distinct regions are consistent with the formation of thermodynamically distinct “condensed complexes” between cholesterol and phospholipids (23). In this model, immiscibility in the  $\alpha$ -region (at low cholesterol) is the result of demixing between complexes and phospholipids, whereas immiscibility in the  $\beta$ -region is the result of demixing between complexes and cholesterol or other sterols.

Here we explore the monolayer phase behavior of dipalmitoyl phosphatidylcholine (DPPC) mixed with a variety of sterols (Fig. 2) over a broad range of compositions.

Submitted August 19, 2005, and accepted for publication January 5, 2006.

Address reprint requests to Sarah L. Keller, E-mail: slkeller@chem.washington.edu.

© 2006 by the Biophysical Society

0006-3495/06/05/3176/08 \$2.00

doi: 10.1529/biophysj.105.072959

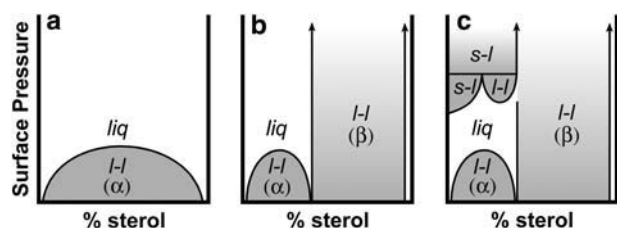


FIGURE 1 Progression of phase diagrams determined by epifluorescence microscopy of monolayers containing phospholipids and sterols. (a) Sketch of early reports of immiscibility for a binary system (e.g., DOPC and dihydrocholesterol (20)), with a shaded region of coexisting liquid phases (*l-l*) at low surface pressure, and one uniform liquid phase (*liq*) at higher pressures. (b) Sketch showing two distinct shaded regions of coexisting liquid phases: the  $\alpha$ -region at low cholesterol and the  $\beta$ -region at high cholesterol (e.g., DPPC and dihydrocholesterol (22)). (c) Sketch showing five distinct shaded regions of coexisting phases, either solid-liquid (*s-l*) or liquid-liquid (*l-l*) (e.g., DMPS/GM1/dihydrocholesterol (45)).

We find that the bilayer classification of sterols as either membrane active or inactive often (though not infallibly) predicts the miscibility phase behavior of sterol/phospholipid monolayers. We also find that the monolayer phase diagrams contain distinct  $\alpha$ - and  $\beta$ -regions of immiscible liquid phases. Finally, we report novel lipid phase behavior of both an upper and a lower critical point for monolayers containing 25-hydroxycholesterol, an oxysterol known to regulate cholesterol homeostasis (12,24,25). The lower miscibility transition correlates with an abrupt change of slope in the monolayer pressure-area isotherm. This is interesting because although a change in monolayer compressibility at the upper miscibility transition has long been expected and has been found for select lipid compositions (26–28), no general correlation has been subsequently confirmed (29).

## METHODS AND MATERIALS

DPPC and dioleoyl phosphocholine (DOPC) were obtained from Avanti Polar Lipids (Alabaster, AL). Cholesterol (5-cholesten-3 $\beta$ -ol), 25-hydroxycholesterol, desmosterol, dihydrocholesterol (5 $\alpha$ -cholestan-3 $\beta$ -ol), ergosterol, lanosterol, and lathosterol were obtained from Sigma-Aldrich (St. Louis, MO). Androstenedione (5-androsten-3 $\beta$ -ol-17-one), cholestane (5 $\alpha$ -cholestane), cholestenone (4-cholesten-3-one), coprostanol (5 $\beta$ -cholestan-3 $\beta$ -ol), and epicholesterol (5-cholesten-3 $\alpha$ -ol) were obtained from Steraloids (Newport, RI). All sterols were purchased as dry powders and used without further purification. Lipid stock solutions were mixed at 1–10 mg/ml in high-performance liquid chromatography-grade chloroform and stored at  $-20^{\circ}\text{C}$  until use. In most cases, lipid mixtures were prepared at 0.25 mg/ml and stored in 1 ml volumetric flasks. Monolayers were deposited on a subphase of purified water of resistivity  $>18\text{ M}\Omega\text{ cm}$  (Barnstead, Dubuque, IA).

The fluorescent probe Texas red dipalmitoyl-phosphatidylethanolamine (TR-DPPE, Molecular Probes, Eugene, OR) was included at 0.5 mol % to provide contrast between immiscible lipid phases as described elsewhere (6). Although other researchers have shown that monolayer transition pressures are not affected by the addition of 0.5 mol % dye (28), the presence of dye and any impurities resident in purchased lipids or sterols always has the potential to alter miscibility transition pressures. Even “pure” DPPC monolayers exhibit solid-liquid coexistence over a range of surface pressures,

rather than at only one pressure as would be expected for an ideal single component system by the Gibbs Phase Rule.

Lipid monolayer surface pressures were measured at the air-water interface with a Wilhelmy plate (Riegler & Kirstein, Berlin, Germany) using a home-built Langmuir trough similar to troughs previously described (30,31). Lipid monolayers were imaged using a Nikon Y-FL microscope (Melville, NY) and a CoolSnap FX charge-coupled device camera (Roper, Princeton, NJ). Isotherm data were taken  $\sim 4$  min after deposition of lipids at the air-water interface. To establish consistency between isotherm measurements and fluorescence microscopy measurements, all samples contained TR-DPPE. Experiments were conducted at room temperature ( $23.5^{\circ}\text{C} \pm 1^{\circ}\text{C}$ ). Monolayers contained 10–60 mol % sterol. At sterol concentrations  $<10$  mol %, domains are small and difficult to image. To prevent monolayer exposure to air and ozone (31–34), our entire experimental apparatus was enclosed in an argon-filled glove bag.

## Identifying two-phase regions

At low surface pressures, lipid monolayers of sterol/DPPC mixtures separate into two distinct regions of coexisting liquid phases, called the  $\alpha$ -region at low cholesterol and the  $\beta$ -region at high cholesterol. Using fluorescence microscopy, the  $\alpha$ -region and its corresponding transition pressures are easily identified. As the surface pressure is lowered, a uniform monolayer abruptly demixes into two coexisting liquid phases. The error in determining transition pressures for the  $\alpha$ -region is typically  $\pm 0.5\text{ mN/m}$ .

The exact boundaries of the  $\beta$ -region are not as easily identified in terms of surface pressure and composition, as represented by the upward arrows in Fig. 1. Here we note only whether or not domains that correspond to the  $\beta$ -region are seen, and not what their transition pressures are. Our previously described criteria to identify the  $\beta$ -region are repeated here for completeness (31).

1. Domains in the  $\beta$ -region persist at surface pressures much greater than in the  $\alpha$ -region. At high pressures, these domains are sparsely and unevenly distributed throughout the monolayer.
2. At high pressures, the fluorescence contrast often inverts from bright domains on a dark background to the opposite (22).
3. As the surface pressure is lowered below  $\sim 5\text{--}15\text{ mN/m}$ , the sparse, bright domains are suddenly joined by uniformly dispersed small bright domains.

## Isotherm analysis

At least two isotherms were collected for each composition, and representative isotherms are shown here. Molecular areas of the Langmuir trough are stable to within  $\sim 2\text{ \AA}^2$ , where error is a function of sample composition and deposition technique. Trough electronics and system have been described elsewhere (31,35). Monolayer compressibility,  $C$ , is defined as  $C = (-1/A)(dA/d\Pi)$ , where  $A$  = molecular area and  $\Pi$  = surface pressure.

## RESULTS

We produced monolayers of the phospholipid DPPC mixed with each of the sterols in Fig. 2. The first six sterols in the figure satisfy Barenholz’s definition of membrane active including cholesterol, epicholesterol, lathosterol, dihydrocholesterol, ergosterol, and desmosterol. From previous reports, we expect monolayers containing cholesterol to be similar to monolayers containing dihydrocholesterol (20). We subsequently found that all membrane-active sterols in

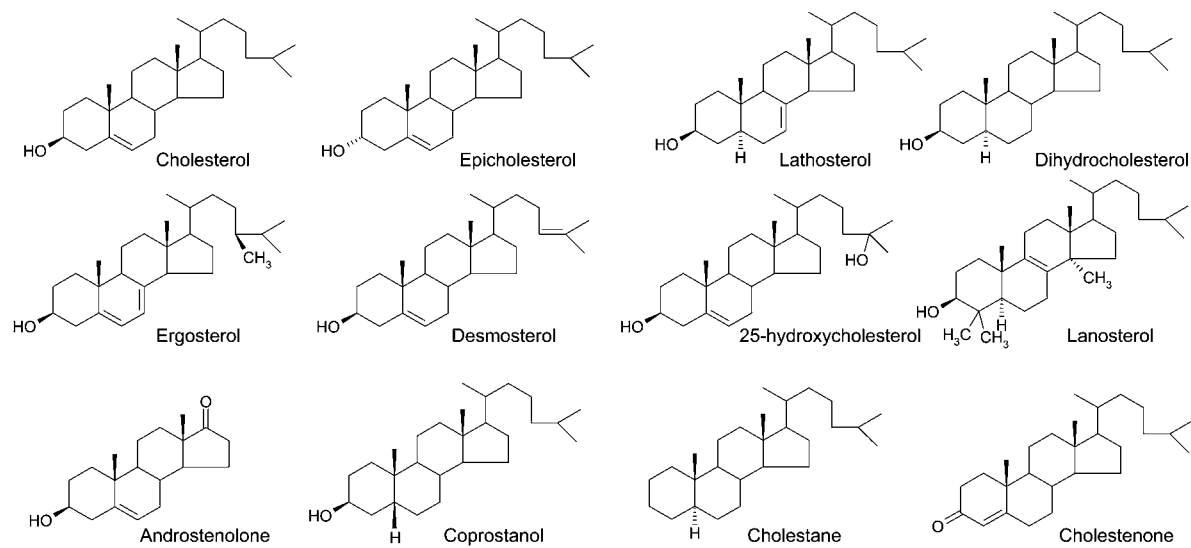


FIGURE 2 All sterols and steroids here share a common structural element of three 6-carbon rings fused to a 5-carbon ring.

the group enable the formation of liquid domains in monolayers with DPPC (Table 1 and Fig. 3). All membrane-active sterols produce phase diagrams similar to that sketched in Fig. 1 b, corresponding to two distinct regions of immiscible liquid phases, the  $\alpha$ -region at low cholesterol and the  $\beta$ -region at high cholesterol. All of our  $\alpha$ -regions have transition pressures below 13 mN/m (sometimes vanishingly low) as seen previously in mixtures of DPPC with either cholesterol (28,36) or dihydrocholesterol (37). We would expect that replacing or augmenting DPPC with a phospho-

lipid that has shorter, branched, or unsaturated chains would increase the transition pressure in the  $\alpha$ -region (28,38,39). As evidence of this, Fig. 4 shows a ternary phase diagram for monolayers containing DPPC, cholesterol, and DOPC. Within the  $\alpha$ -region, transition pressures are low for the binary system of sterol and DPPC (along the right axis), higher for the binary system of sterol and DOPC (along the left axis), and highest for ternary mixtures with roughly equimolar concentrations of the two phospholipids. Although the trend between shorter or unsaturated phospholipid chains and higher

TABLE 1 Summary of sterol results

Sterol	Membrane active	Liquid-liquid at low sterol ( $\alpha$ -region)	Liquid-liquid at high sterol ( $\beta$ -region)	Molecular area at 2 mN/m ( $\pm 2 \text{ \AA}^2$ )	Molecular area at 12 mN/m ( $\pm 2 \text{ \AA}^2$ )	Collapse pressure ( $\pm 1 \text{ mN/m}$ )	Molecular area at collapse ( $\pm 2 \text{ \AA}^2$ )
Cholesterol	Yes	Yes	Yes	38 $\text{\AA}^2$	37 $\text{\AA}^2$	40 mN/m	36 $\text{\AA}^2$
Epicholesterol	Yes	No	Yes	42 $\text{\AA}^2$	41 $\text{\AA}^2$	35 mN/m	40 $\text{\AA}^2$
Lathosterol	Yes	No	Yes	37 $\text{\AA}^2$	37 $\text{\AA}^2$	52 mN/m	36 $\text{\AA}^2$
Dihydrocholesterol	Yes	Yes	Yes	37 $\text{\AA}^2$	37 $\text{\AA}^2$	34 mN/m	36 $\text{\AA}^2$
Ergosterol	Yes	Yes	Yes	40 $\text{\AA}^2$	37 $\text{\AA}^2$	49 mN/m	35 $\text{\AA}^2$
Desmosterol	Yes	Yes	Yes	33 $\text{\AA}^2$	32 $\text{\AA}^2$	27 mN/m	32 $\text{\AA}^2$
25-Hydroxysterol	No	Yes	Yes	40 $\text{\AA}^2$	39 $\text{\AA}^2$	28 mN/m	37 $\text{\AA}^2$
Lanosterol	No	No	No	N/A	N/A	N/A	N/A
Androstenedione	No	No	No	N/A	N/A	N/A	N/A
Coprostanol	No	No	No	45 $\text{\AA}^2$	44 $\text{\AA}^2$	42 mN/m	41 $\text{\AA}^2$
Cholestane	No	Yes	No	N/A	N/A	N/A	N/A
Cholestanone	No	No	No	60 $\text{\AA}^2$	53 $\text{\AA}^2$	28 mN/m	46 $\text{\AA}^2$

Sterols that fit Barenholtz's membrane-active criteria generally produce coexisting liquid phases in monolayers containing DPPC. The asterisk indicates that cholestane is squeezed out of the monolayer so that high sterol concentrations cannot be obtained. The table also records details from isotherms of pure sterol monolayers, including molecular areas, and the monolayer surface pressure at collapse. Monolayers of pure androstenedione, lanosterol, and cholestane are not stable, which is denoted by "N/A". When available, previous data for molecular areas of pure sterol monolayers at 12 mN/m ( $\text{Area}_{12}$ ) tend to be consistent with our results to within our error of  $\pm 2 \text{ \AA}^2$ , whereas we find collapse pressures ( $\Pi_c$ ) consistently higher than those reported in the literature. For example, when deposited on a pure water subphase at 22°C, cholesterol has  $\text{Area}_{12} = 39.0 \text{ \AA}^2/\text{molecule}$  and  $\Pi_c = 37.2 \text{ mN/m}$ , epicholesterol has  $\text{Area}_{12} = 40.2 \text{ \AA}^2/\text{molecule}$  and  $\Pi_c = 26.5 \text{ mN/m}$ , lathosterol has  $\text{Area}_{12} = 38.5 \text{ \AA}^2/\text{molecule}$  and  $\Pi_c = 41.0 \text{ mN/m}$ , ergosterol has  $\text{Area}_{12} = 38.5 \text{ \AA}^2/\text{molecule}$  and  $\Pi_c = 31.7 \text{ mN/m}$ , coprostanol has  $\text{Area}_{12} = 43.8 \text{ \AA}^2/\text{molecule}$  and  $\Pi_c = 33.6 \text{ mN/m}$ , and cholestanone has  $\text{Area}_{12} = 50 \text{ \AA}^2/\text{molecule}$ , and  $\Pi_c = 27.4 \text{ mN/m}$  (63) or  $\Pi_c = 27 \text{ mN/m}$  with a collapse area of  $40 \text{ \AA}^2/\text{molecule}$  (44). Under different conditions of a buffered subphase at 37°C, cholesterol's collapse pressure changed to 43.5 mN/m at a collapse area of  $35.0 \pm 1.2 \text{ \AA}^2/\text{molecule}$ , and desmosterol's collapse pressures was 36.1 mN/m at a collapse area of  $33.6 \pm 1.2 \text{ \AA}^2/\text{molecule}$  (64).

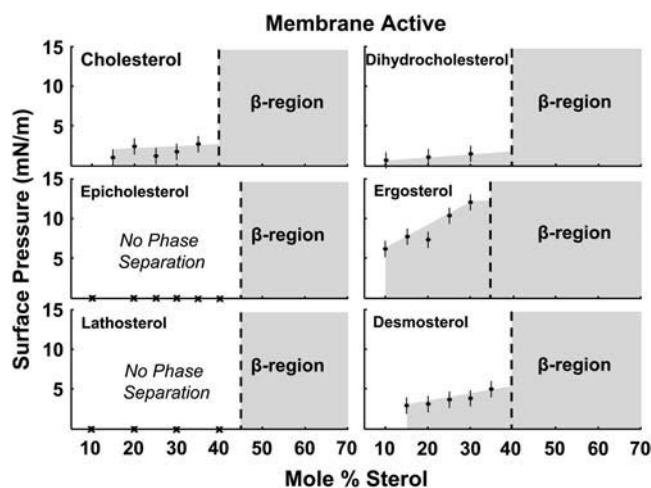


FIGURE 3 Phase diagrams for monolayers of DPPC containing membrane-active sterols. Regions of immiscible liquid phases are shaded: the  $\alpha$ -region at low cholesterol and the  $\beta$ -region at high cholesterol. No attempt was made to identify solid phases at high surface pressure (compare with Fig. 1 *c*) or to explore sterol concentrations <10 mol % or >70 mol %. Concentrations at which no coexisting phases were observed are denoted by “x” symbols along the *x* axis.

$\alpha$ -region transition pressures is well documented (28,38,39), we can offer no similar obvious trend between the structures of the membrane-active sterols in Fig. 2 and the  $\alpha$ -region transition pressures in Fig. 3. The  $\alpha$ -region gives way to a  $\beta$ -region at sterol compositions of  $\sim 35$ – $45\%$ . This range is not significant within our errors given our resolution.

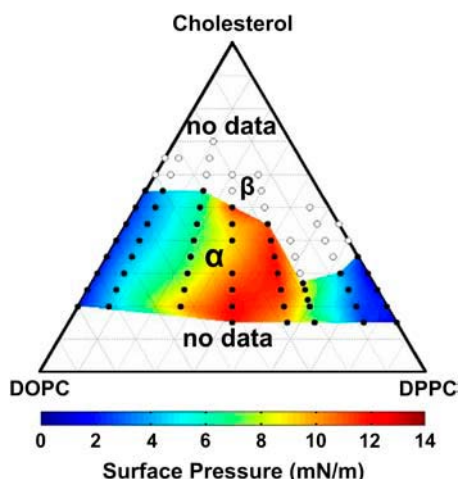


FIGURE 4 Ternary phase diagram for monolayers containing DOPC, DPPC, and cholesterol (31). Two different regions of immiscible liquid phases are observed, the  $\alpha$ -region at low cholesterol (●) and the  $\beta$ -region at high cholesterol (○). Transition pressures in the  $\alpha$ -region are recorded in color, and regions between points are calculated by a polynomial fit. Transition pressures in the  $\alpha$ -region are highest near equimolar ratios of the two phospholipids, DOPC and DPPC. Transition pressures in the  $\beta$ -region are greater than in the  $\alpha$ -region, often well above 15 mN/m. Regions with no symbols represent regions of the phase diagram that were not investigated (rather than regions with no coexisting liquid phases).

Sterols that do not satisfy Barenholz’s definition of membrane active appear at the bottom of Fig. 2 and include 25-hydroxycholesterol, lanosterol, androstenolone, coprostanol, cholestane, and cholestenone. Four of the six of these membrane-inactive sterols do not form coexisting liquid phases when mixed with DPPC (Table 1 and Fig. 5). Although these sterols do not produce liquid phases, they do perturb the solid phase of DPPC. In the absence of any sterol, monolayers of pure DPPC undergo a liquid to solid transition as surface pressure increases above  $\sim 7$  mN/m. Evidence of the transition is observed in the formation of solid domains by fluorescence microscopy (Fig. 6 *b*) and in a plateau in the pressure-area isotherm (40). When small amounts of cholesterol are added to the DPPC monolayer, the liquid-solid transition pressure increases (as sketched in Fig. 1 *c*) and the perimeter of the solid domains increases, implying that cholesterol stabilizes the solid-liquid interface (41). We observe the same effect when coprostanol is added to a DPPC monolayer (Fig. 6 *a*).

Moving on to the remaining sterols, 25-hydroxycholesterol does not satisfy the membrane active criteria because it terminates in an alcohol rather than an alkyl tail. 25-Hydroxycholesterol seems to defy its classification because monolayers containing 25-hydroxycholesterol produce both  $\alpha$ - and  $\beta$ -regions of immiscibility just as the membrane-active sterols do (Fig. 5). The phase diagram of 25-hydroxycholesterol is doubly interesting because the  $\alpha$ -region contains both an upper and a lower immiscibility transition, and the lower transition corresponds to an abrupt change of slope in the pressure-area isotherm (Fig. 7). Correlations between miscibility transitions and monolayer compressibility have long been predicted and have been reported for limited lipid compositions but to our knowledge have never been unambiguously verified (26–29).

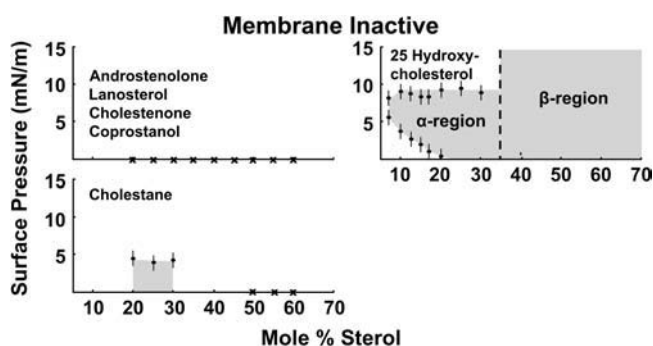


FIGURE 5 Phase diagrams for monolayers of DPPC-containing membrane-inactive sterols. Monolayers containing androstenolone, lanosterol, cholestenone, and coprostanol exhibit no liquid-liquid immiscibility for all concentrations studied (denoted by “x” symbols) along the *x* axis. In contrast, monolayers containing 25-hydroxycholesterol exhibit two distinct regions of immiscibility: an  $\alpha$ -region at low sterol and a  $\beta$ -region at high sterol. The  $\alpha$ -region is bounded by both an upper and a lower miscibility transition. At low cholesterol concentrations, monolayers form two liquid phases, but cholestane is squeezed out of the monolayer at higher concentrations (see Fig. 9).

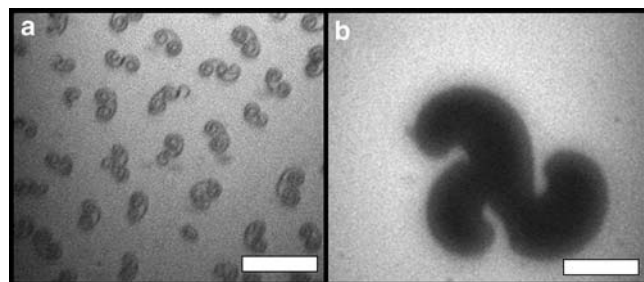


FIGURE 6 Solid domains in a background of a liquid phase in a monolayer of (a) 4:1 DPPC/coprostanol at  $\sim 9$  mN/m and (b) 100% DPPC at  $\sim 9$  mN/m (plus 0.5% TR-DPPE). The addition of coprostanol increases the perimeter of solid domains. Scale bar  $20\ \mu\text{m}$ .

Monolayers containing 25-hydroxycholesterol are also distinguished by an unexpected increase in molecular area as sterol concentration increased from 10 to 20 mol % (below surface pressures of 1.5 mN/m; data not shown). Similarly, the molecular area at which the first nonzero surface pressure is measured (the “lift off” area) is highest for monolayers containing 10–20 mol % of 25-hydroxycholesterol among the dozen sterols and steroids investigated. This high lift off area is reflected in large molecular areas for 25-hydroxycholesterol at 5 mN/m as shown in Fig. 8 *a*. These results are consistent with a model in which 25-hydroxycholesterol lies more flat at the air-water interface because it possesses hydrophilic moieties at both ends of the molecule. We have no knowledge of whether 25-hydroxycholesterol flips in the monolayer or whether a flip would account for the observed phase behavior. 25-Hydroxycholesterol was the only oxysterol in our study.

Cholestane is the last sterol that does not fit into the membrane active criteria. The reason is obvious. Cholestane has no hydrophilic groups, so it is not well anchored at the

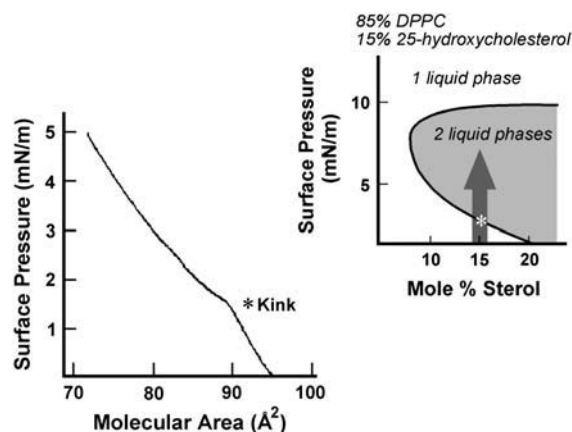


FIGURE 7 Pressure-area isotherm of a monolayer containing 85 mol % DPPC and 15 mol % 25-hydroxycholesterol (with 0.5 mol % TR-DPPE). A kink in the isotherm (at the asterisk) corresponds to the lower miscibility transition sketched in the inset. The full phase diagram of DPPC/25-hydroxycholesterol is found in Fig. 5.

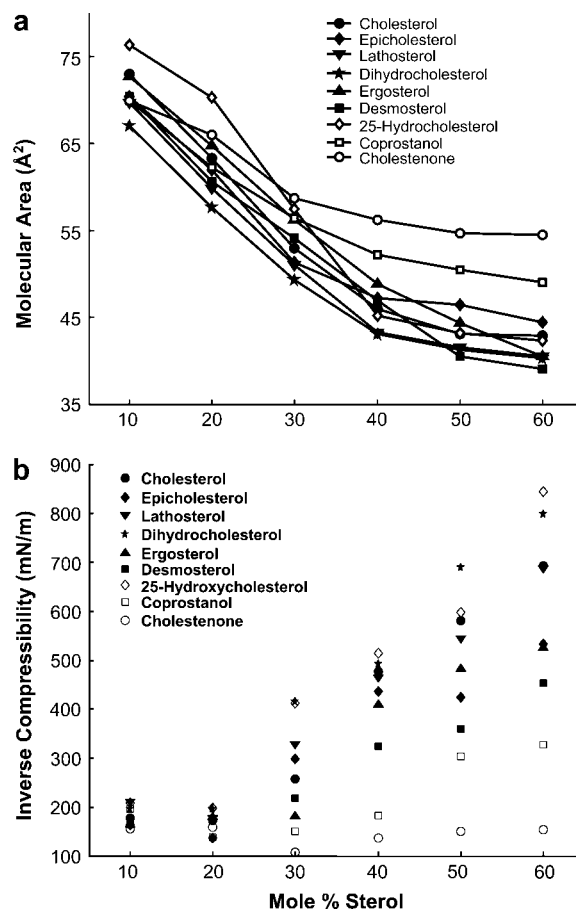


FIGURE 8 (a) Molecular areas for isobaric cuts at 5 mN/m through pressure-area isotherms of DPPC/sterol monolayers. Errors are  $\pm 2\ \text{\AA}^2$ . (b) Inverse compressibilities calculated from pressure-area isotherms at 25 mN/m. As membrane-active sterol composition increases in lipid monolayers, so does the inverse compressibility. Inverse compressibilities are lowest for membrane-inactive sterols (open symbols), with the exception of 25-hydroxycholesterol.

air-water interface. At high surface pressures or high cholestane concentrations, monolayers suffer a decrease in molecular area (Fig. 9). Cholestane is likely squeezed out and lies above the hydrophobic face of the monolayer. Liquid-liquid coexistence is unambiguously observed only in monolayers with mole fractions of cholestane below  $\sim 30\%$ , for which the steroid still resides in the monolayer (Fig. 5). For contrast, a set of pressure-area isotherms typical of the other sterols (e.g., desmosterol) also appears in Fig. 9. As sterol concentration increases, the plateau due to solid-liquid coexistence becomes less prominent and the monolayer becomes less compressible.

Isotherm data for all pure sterol monolayers are recorded in Table 1. Isobaric cuts were taken through DPPC/sterol isotherms at 5 mN/m (Fig. 8). As expected, increases in sterol concentration result in decreases in average molecular area. Fig. 8 *b* shows inverse compressibilities for all stable monolayers at 25 mN/m. With the notable exception of

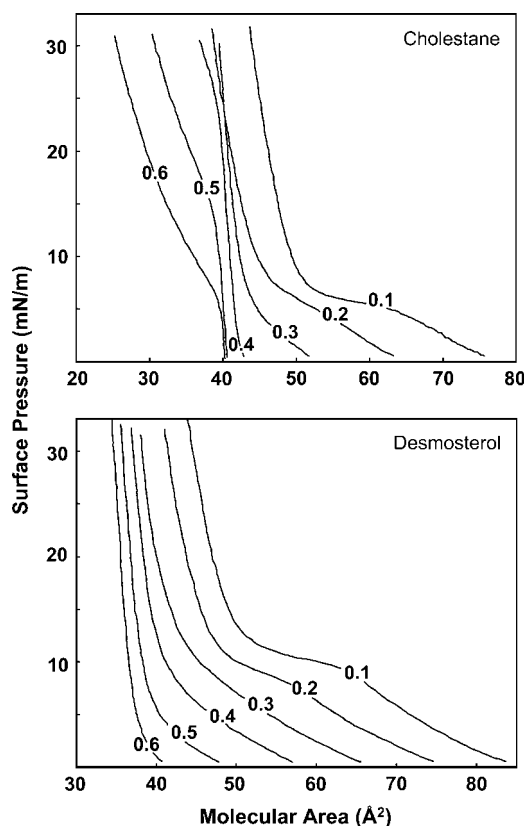


FIGURE 9 Pressure-area isotherms of monolayers containing DPPC and either cholestane (*top*) or desmosterol (*bottom*) at the mole fractions labeled on each curve. At concentrations  $\geq 40$  mol %, cholestane is squeezed out of the monolayer. In contrast, desmosterol isotherms show no evidence of squeeze-out. The plateau at  $\sim 7$  mN/m for cholestane and  $\sim 10$  mN/m for desmosterol marks the onset of gel (*solid*) domains as in Fig. 6.

25-hydroxycholesterol, membrane-active sterols have higher inverse compressibilities than membrane-inactive sterols. These results are consistent with the observation that the substitution of cholesterol with lathosterol, 7-dehydrocholesterol, and lanosterol in DPPC bilayers reduces membrane rigidity (5).

## DISCUSSION

Sterols that produce coexisting liquid phases in monolayers of DPPC are generally those that fit Barenholz's criteria for membrane-active sterols. This establishes a correlation between lipid monolayers and bilayers. We previously found that membrane-active sterols typically form coexisting liquid phases in vesicles of DOPC/DPPC/sterol (18). The membrane active classification generally agrees with London's classification of "promoter" and "inhibitor" sterols based on their ability to enhance or diminish the amount of DPPC-rich phase in bilayers as measured by fluorescence quenching in vesicle systems (42). Taken most optimistically, our results suggest that similar sterol/phospholipid interactions may

cause phase separation in both monolayers and in bilayers. However, the compositions and molecular areas over which coexisting liquid phases are observed clearly do not correlate well between monolayer and bilayer systems, implying that transbilayer and dipole interactions play an important role in phase separation (31).

Now consider the sterols that fail Barenholz's membrane active criteria. Pure monolayers of androstenolone, lanosterol, and cholestane are all unstable. These sterols also fail to form coexisting liquid domains in DOPC/DPPC/sterol mixtures (18). It is reasonable to conclude that if the sterol or steroid molecule is not stable at the air-water interface, then it is unlikely to align strongly with and interact strongly with lipids in bilayers.

We are not the first to investigate alternate sterols in lipid monolayers. Studies of cholesterol analogs with alkyl chain lengths from 3 to 10 carbons have shown that a chain of at least 5 carbons is required to produce coexisting liquid domains in DPPC monolayers (43). The position of the sterol's double bond and the moiety at the 3-position also determine miscibility behavior (44). Two distinct regions of phase separation have been reported for monolayers containing DPPC with 20 mol % short chain cholesterol analogs (43), but the specific phases present were not reported (e.g., solid-liquid phase separation versus liquid-liquid). Phase diagrams containing two regions of liquid immiscibility, the  $\alpha$ -region and  $\beta$ -region, with two upper critical points have been previously reported in monolayers containing either cholesterol or dihydrocholesterol (21).

One aim of this work was to test if cholesterol and dihydrocholesterol were the only two sterols capable of producing two regions of liquid-liquid immiscibility in phospholipid monolayers. Since many sterols produce similar phase diagrams, it is unlikely that the ability to form two regions of immiscibility is one of the biophysical attributes that explains cholesterol's predominance in animal membranes.

If the observation of two regions of immiscibility is a consequence of the formation of "condensed complexes", then many sterols possess this property when mixed with DPPC. The lack of an  $\alpha$ -region for epicholesterol and lathosterol is in line with a model in which complexes exist but do not phase separate from pure DPPC. Our phase diagrams are consistent with the condensed complexes model, even though our data of molecular areas do not provide direct evidence for complexes. Within our gaps between data points of 5 mol % sterol and resolution of  $\pm 2 \text{ \AA}^2$  in molecular area in Fig. 8, we find no minimum in molecular area at 35–45 mol % sterol corresponding to the onset of the  $\alpha$ -region and the highest membrane concentration of condensed complex (see (23,31, 45,46)). Our observation of regions of immiscibility is consistent with a variety of theories similar to the condensed complexes model, namely superlattice models (47–50), mean-field models of liquid-ordered phases (51), and microscopic molecular models (52,53). For researchers wishing to

specifically test the condensed complexes model, we recommend an alternate experiment in which the chemical activities of sterols in monolayers are found by evaluating the rate at which  $\beta$ -cyclodextrin desorbs sterol from the air-water interface (46). A single stoichiometry of the complex (or a single equivalence point) would be confirmed by a single, sharp increase in the sterol desorption rate at the sterol composition dividing the  $\alpha$ - and  $\beta$ -regions.

Our current and previous work with various sterols is motivated by a desire not only to investigate the biophysical attributes of sterols, but also to assist theorists currently modeling membranes containing sterols. Both monolayers and bilayers are amenable to simulations. Our results can be applied to atomistic-level molecular dynamics simulations of membranes containing lipids and cholesterol (54), which in turn provide membrane material properties used in continuum models of domains in giant unilamellar vesicles (55). Atomistic simulations have also been employed to study the distribution of sterol, saturated lipids, and unsaturated lipids around a membrane protein such as rhodopsin, in which the interactions of cholesterol with lipid chains is thought to stabilize the native form of the protein (56). We hope that our cumulative results will be useful for refining interaction parameters and force fields between lipids and cholesterol within the plane of the membrane (51,57–61) and for calculating the profile of bilayer thickness due to the presence of membrane inclusions by sterols (62).

We thank Dr. Sarah Veatch and Dr. Michael Halter for helpful discussions. Research in the Keller laboratory is supported by a National Science Foundation Career Award (MCB-0133484), a Research Corporation Innovation Award, and a Cottrell Scholar Award.

## REFERENCES

- Nes, W. R. 1974. Role of sterols in membranes. *Lipids*. 9:596–612.
- Nielsen, M., J. Thewalt, L. Miao, J. H. Ipsen, M. Bloom, M. J. Zuckermann, and O. G. Mouritsen. 2000. Sterol evolution and the physics of membranes. *Europhys. Lett.* 52:368–374.
- Huster, D., K. Arnold, and K. Gawrisch. 1998. Influence of docosahexanoic acid and cholesterol on lateral lipid organization in phospholipid mixtures. *Biochemistry*. 37:17299–17308.
- Haines, T. H. 2001. Do sterols reduce proton and sodium leaks through lipid bilayers? *Prog. Lipid Res.* 40:299–324.
- Petrache, H. I., D. Harries, and V. A. Parsegian. 2004. Alteration of lipid membrane rigidity by cholesterol and its metabolic precursors. *Macromol. Symp.* 219:39–50.
- Veatch, S. L., and S. L. Keller. 2002. Organization in lipid membranes containing cholesterol. *Phys. Rev. Lett.* 89:268101.
- Bloch, K. 1991. Cholesterol: evolution of structure and function. In *Biochemistry of Lipids, Lipoproteins, and Membranes*. D. E. Vance and J. Vance, editors. Elsevier, Amsterdam. 363–381.
- Bloom, M., and O. G. Mouritsen. 1988. The evolution of membranes. *Can. J. Chem.* 66:706–712.
- Kelley, R. I., and G. E. Herman. 2001. Inborn errors of sterol biosynthesis. *Annu. Rev. Genomics Hum. Genet.* 2:299–341.
- Chevy, F., F. Illien, C. Wolf, and C. Roux. 2002. Limb malformations of rat fetuses exposed to a distal inhibitor of cholesterol biosynthesis. *J. Lipid Res.* 43:1192–1200.
- Fliesler, S. J., N. S. Peachey, M. J. Richards, B. A. Nagel, and D. K. Vaughan. 2004. Retinal degeneration in a rodent model of Smith-Lemli-Opitz syndrome. *Arch. Ophthalmol.* 122:1190–1200.
- Radhakrishnan, A., L.-P. Sun, H. J. Kwon, M. S. Brown, and J. L. Goldstein. 2004. Direct binding of cholesterol to the purified membrane region of SCAP: mechanism for a sterol-sensing domain. *Mol. Cell.* 15:259–268.
- Wang, J., Megha, and E. London. 2004. Relationship between sterol/steroid structure and participation in ordered lipid domains (lipid rafts): implications for lipid raft structure and function. *Biochemistry*. 43:1010–1018.
- Dietrich, C., L. A. Bagatolli, Z. N. Volovky, N. L. Thompson, M. Levi, K. Jacobson, and E. Gratton. 2001. Lipid rafts reconstituted in model membranes. *Biophys. J.* 80:1417–1428.
- Samsonov, A. V., I. Mihalyov, and F. S. Cohen. 2001. Characterization of cholesterol-sphingomyelin domains and their dynamics in bilayer membranes. *Biophys. J.* 81:1486–1500.
- Veatch, S. L., and S. L. Keller. 2003. Separation of liquid phases in giant unilamellar vesicles of ternary mixtures of phospholipids and cholesterol. *Biophys. J.* 85:3074–3083.
- Bacia, K., P. Schwille, and T. Kurzchalia. 2005. Sterol structure determines the separation of phases and the curvature of the liquid-ordered phase in model membranes. *Proc. Natl. Acad. Sci. USA*. 102:3272–3277.
- Beattie, M. E., S. L. Veatch, B. L. Stottrup, and S. L. Keller. 2005. Sterol structure determines miscibility vs. melting transitions in lipid vesicles. *Biophys. J.* 89:1760–1768.
- Barenholz, Y. 2002. Cholesterol and other membrane active sterols: from membrane evolution to “rafts”. *Prog. Lipid Res.* 41:1–5.
- Hagen, J. P., and H. M. McConnell. 1997. Liquid-liquid immiscibility in lipid monolayers. *Biochim. Biophys. Acta*. 1329:7–11.
- Radhakrishnan, A., and H. M. McConnell. 1999. Cholesterol-phospholipid complexes in membranes. *J. Am. Chem. Soc.* 121:486–487.
- Okonogi, T. M., and H. M. McConnell. 2004. Contrast inversion in the epifluorescence of cholesterol-phospholipid monolayers. *Biophys. J.* 86:880–890.
- Radhakrishnan, A., and H. M. McConnell. 1999. Condensed complexes of cholesterol and phospholipids. *Biophys. J.* 77:1507–1517.
- Hall, A. M., L. Krishnamoorthy, and S. J. Orlow. 2004. 25-hydroxy-cholesterol acts in the Golgi compartment to induce degradation of tyrosinase. *Pigment Cell Res.* 17:396–406.
- Adams, C. M., J. Reitz, J. K. De Brabander, J. D. Feramisco, L. Li, M. S. Brown, and J. L. Goldstein. 2004. Cholesterol and 25-hydroxy-cholesterol inhibit activation of SREBPs by different mechanisms, both involving SCAP and Insigs. *J. Biol. Chem.* 279:52772–52780.
- Albrecht, O., H. Gruler, and E. Sackmann. 1981. Pressure-composition phase diagrams of cholesterol/lecithin, cholesterol/phosphatidic acid, and lecithin/phosphatidic acid mixed monolayers: a Langmuir film balance study. *J. Colloid Interface Sci.* 79:319–338.
- Hirshfeld, C. L., and M. Seul. 1990. Critical mixing in monomolecular films—pressure-composition phase-diagram of a 2-dimensional binary mixture. *J. Phys. [E]*. 51:1537–1552.
- Slotte, J. P. 1995. Lateral domain heterogeneity in cholesterol/phosphatidylcholine monolayers as a function of cholesterol concentration and phosphatidylcholine acyl chain length. *Biochim. Biophys. Acta*. 1238:118–126.
- Keller, S. L. 2003. Miscibility transitions and lateral compressibility in liquid phases of lipid bilayers. *Langmuir*. 19:1451–1456.
- Halter, M., Y. Nogata, O. Dannenberger, T. Sasaki, and V. Vogel. 2004. Engineered lipids that cross-link the inner and outer leaflets of lipid bilayers. *Langmuir*. 20:2416–2423.
- Stottrup, B. L., D. S. Stevens, and S. L. Keller. 2005. Miscibility of ternary mixtures of phospholipids and cholesterol in monolayers, and application to bilayer systems. *Biophys. J.* 88:269–276.
- Benvegnu, D. J., and H. M. McConnell. 1993. Surface dipole densities in lipid monolayers. *J. Phys. Chem.* 97:6686–6691.

33. Lai, C. C., S. H. Yang, and B. J. Finlayson-Pitts. 1994. Interactions of monolayers of unsaturated phosphocholines with ozone at the air-water interface. *Langmuir*. 10:4637–4644.
34. Stottrup, B. L., S. L. Veatch, and S. L. Keller. 2004. Nonequilibrium behavior in supported lipid membranes containing cholesterol. *Biophys. J.* 86:2942–2950.
35. Baneyx, G., and V. Vogel. 1999. Self-assembly of fibronectin into fibrillar networks underneath dipalmitoyl phosphatidylcholine monolayers: role of lipid matrix and tensile forces. *Proc. Natl. Acad. Sci. USA*. 96:12518–12523.
36. Berring, E. E., K. Borenphol, S. J. Fliesler, and A. B. Serfis. 2005. A comparison of the behavior of cholesterol and selected derivatives in mixed sterol-phospholipid Langmuir monolayers: a fluorescence microscopy study. *Chem. Phys. Lipids*. 136:1–12.
37. Perkovic, S., and H. M. McConnell. 1997. Cloverleaf monolayer domains. *J. Phys. Chem. B*. 101:381–388.
38. Keller, S. L., A. Radhakrishnan, and H. M. McConnell. 2000. Saturated phospholipids with high melting temperatures form complexes with cholesterol in monolayers. *J. Phys. Chem.* 104:7522–7527.
39. Keller, S. L., T. G. Anderson, and H. M. McConnell. 2000. Miscibility critical pressures in monolayers of ternary lipid mixtures. *Biophys. J.* 79:2033–2042.
40. Hunt, R. D., M. L. Mitchell, and R. A. Dluhy. 1989. The interfacial structure of phospholipid monolayer films—an infrared reflectance study. *J. Mol. Struct.* 214:93–109.
41. McConnell, H. M. 1991. Structures and transitions in lipid monolayers at the air-water interface. *Annu. Rev. Phys. Chem.* 42:171–195.
42. Xu, X., and E. London. 2000. The effect of sterol structure on membrane lipid domains reveals how cholesterol can induce lipid domain formation. *Biochemistry*. 39:843–849.
43. Mattjus, P., R. Bittman, C. Vilcheze, and J. P. Slotte. 1995. Lateral domain formation in cholesterol phospholipid monolayers as affected by the sterol side chain conformation. *Biochim. Biophys. Acta*. 1240:237–247.
44. Slotte, J. P. 1995. Effect of sterol structure on molecular interactions and lateral domain formation in monolayers containing dipalmitoyl phosphatidylcholine. *Biochim. Biophys. Acta*. 1237:127–134.
45. Radhakrishnan, A., and H. M. McConnell. 2002. Critical points in charged membranes containing cholesterol. *Proc. Natl. Acad. Sci. USA*. 99:13391–13396.
46. McConnell, H. M., and A. Radhakrishnan. 2003. Condensed complexes of cholesterol and phospholipids. *Biochim. Biophys. Acta*. 1610:159–173.
47. Wang, M. M., I. P. Sugar, and P. L. G. Chong. 1998. Role of the sterol superlattice in the partitioning of the antifungal drug nystatin into lipid membranes. *Biochemistry*. 37:11797–11805.
48. Sugar, I. P., D. X. Tang, and P. L. G. Chong. 1994. Monte-Carlo simulation of lateral distribution of molecules in a 2-component lipid-membrane—effect of long-range repulsive interactions. *J. Phys. Chem.* 98:7201–7210.
49. Virtanen, J. A., M. Ruonala, M. Vauhkonen, and P. Somerharju. 1995. Lateral organization of liquid-crystalline cholesterol-dimyristoylphosphatidylcholine bilayers—evidence for domains with hexagonal and centered rectangular cholesterol superlattices. *Biochemistry*. 34:11568–11581.
50. Somerharju, P., J. A. Virtanen, and K. H. Cheng. 1999. Lateral organization of membrane lipids. The superlattice view. *Biochim. Biophys. Acta*. 1440:32–48.
51. Ipsen, J. H., G. Karlstrom, O. G. Mouritsen, H. Wennerstrom, and M. J. Zuckermann. 1987. Phase equilibria in the phosphatidylcholine-cholesterol system. *Biochim. Biophys. Acta*. 905:162–172.
52. Fraser, D. P., M. J. Zuckermann, and O. G. Mouritsen. 1991. Theory and simulations for hard-disk models of binary-mixtures of molecules with internal degrees of freedom. *Phys. Rev. A*. 43:6642–6656.
53. Miao, L., M. Nielsen, J. Thewalt, J. H. Ipsen, M. Bloom, M. J. Zuckermann, and O. G. Mouritsen. 2002. From lanosterol to cholesterol: structural evolution and differential effects on lipid bilayers. *Biophys. J.* 82:1429–1444.
54. Ayton, G. S., and G. A. Voth. 2004. Simulation of biomolecular systems at multiple length and time scales. *Intl. J. Mult. Comput. Eng.* 2: 291–311.
55. Ayton, G. S., J. L. McWhirter, P. McMurtry, and G. A. Voth. 2005. Coupling field theory with continuum mechanics: a simulation of domain formation in giant unilamellar vesicles. *Biophys. J.* 88:3855–3869.
56. Pitman, M. C., A. Grossfield, F. Suits, and S. E. Feller. 2005. Role of cholesterol and polyunsaturated chains in lipid-protein interactions: molecular dynamics simulation of rhodopsin in a realistic membrane environment. *J. Am. Chem. Soc.* 127:4576–4577.
57. Tu, K., M. L. Klein, and D. J. Tobias. 1998. Constant-pressure molecular dynamics investigation of cholesterol effects in a dipalmitoylphosphatidylcholine bilayer. *Biophys. J.* 75:2147–2156.
58. Huang, J., and G. W. Feigenson. 1999. A microscopic interaction model of maximum solubility of cholesterol in lipid bilayers. *Biophys. J.* 76:2142–2157.
59. Smondyrev, A. M., and M. L. Berkowitz. 2001. Molecular dynamics simulation of the structure of dimyristoylphosphatidylcholine bilayers with cholesterol, ergosterol, and lanosterol. *Biophys. J.* 80:1649–1658.
60. Chiu, S. W., E. Jakobsson, R. J. Mashl, and H. L. Scott. 2002. Cholesterol-induced modifications in lipid bilayers: a simulation study. *Biophys. J.* 83:1842–1853.
61. Hofstätter, C., E. Lindahl, and O. Edholm. 2003. Molecular dynamics simulations of phospholipid bilayers with cholesterol. *Biophys. J.* 84: 2192–2206.
62. Pata, V., and N. Dan. 2005. Effect of membrane characteristics on phase separation and domain formation in cholesterol-lipid mixtures. *Biophys. J.* 88:916–924.
63. Demel, R. A., K. R. Bruckdorfer, and L. L. M. van Deenen. 1972. Structural requirements of sterols for the interaction with lecithin at the air-water interface. *Biochim. Biophys. Acta*. 255:311–320.
64. Serfis, A. B., S. Brancato, and S. J. Fliesler. 2001. Comparative behavior of sterols in phosphatidylcholine-sterol monolayer films. *Biochim. Biophys. Acta*. 1511:341–348.